RAPID COMMUNICATIONS

PHYSICAL REVIEW E VOLUME 48, NUMBER 2 AUGUST 1993

Coexisting traveling waves and steady rolls in binary-fluid convection

Paul Kolodner
AT&T Bell Laboratories, Murray Hill, New Jersey 07974-0636
(Received 31 March 1993)

I present experimental observations of a new state of convection in an ethanol-water mixture with separation ratio $\psi = -0.020$ in a narrow, annular container. Increasing the Rayleigh number to about 1% above the onset of convection causes the system to evolve from the erratic state called "dispersive chaos" into a regime in which bursts of traveling waves coexist with a persistent region of steady convective rolls. Remarkably, the traveling-wave bursts appear at regular intervals. Equally remarkably, the burst frequencies of the two oppositely directed traveling-wave components are different. Evidence for the reflection of traveling waves at the boundaries of the steady-roll region is seen.

PACS number(s): 47.27.Te, 47.20.Bp, 47.20.Ky

Several years ago, experiments on one-dimensional patterns of binary-fluid convection in narrow, rectangular containers revealed a striking, regular, nonlinear state of traveling waves (TW's) just above onset. In that state, amplitude appeared alternately in the two oppositely directed TW components on opposite ends of the container, giving the visual appearance of periodically "blinking" back and forth across the container [1]. The physics of this "blinking" state was elucidated by Cross [2] in a simple coupled-Ginzburg-Landau-equation model: reflections of TW's that approach one end wall of the cell tunnel through the incident TW's. As they grow in amplitude and propagate towards the opposite end wall, they suppress the original TW's through a nonlinear cross coupling. This half-cycle then repeats, leading to regular blinking.

Subsequent experiments on this system have been performed in very long rectangular [3] and annular [4] containers. In rectangles of increasing length, nonlinear growth and dispersion come to dominate the influence of reflections from far end walls and lead to erratic blinking [3]. In unidirectional TW states in an annular container, where there are no reflections, nonlinear dispersion alone can cause irregular behavior close to onset, dubbed "dispersive chaos" [4]. In a related experiment on binary-fluid convection in a long, "slot" container with absorbing ends, erratic behavior caused by the convective amplification of TW fluctuations has also been reported [5].

In this paper, I report observations of binary-fluid convection in an annular container made above the Rayleigh-number domain of dispersive chaos. I observe a reentrant regular state in which a persistent patch of steady convective rolls (SR's) is surrounded by a region in which TW bursts appear at regular intervals. Reflections of TW's from the edges of the SR region are seen. While these observations may sound reminiscent of regular "blinking," they are, in fact, quite different.

The apparatus in which these experiments were performed has recently been described in detail [6]. The cell is an annular channel of height $d = 0.2737$ cm, radial width $1.677d$, and mean circumference $82.47d$, which is formed by a plastic disk and ring that are clamped between a heated, mirror-polished silicon bottom plate and a water-cooled sapphire top plate. The fluid filling the cell is a 0.40-wt % ethanol-water solution at a mean temperature of 27.27 °C, for which the separation ratio $\psi = -0.020$, the Prandtl number $P = 5.97$, and the Lewis number $L = 0.0085$ [7]. The Rayleigh number, quoted herein as the fractional distance above onset, ϵ, is temporally stable to within $\pm 5 \times 10^{-5}$ and spatially uniform to within $\pm 4 \times 10^{-4}$. The flow, consisting of stationary rolls or TW's that propagate azimuthally around the cell (in directions called "left" and "right"), is visualized by shadowgraphy and recorded by an annular array of 720 photodiodes whose output is sampled at regular time intervals by a small computer. These patterns are analyzed using techniques described in Refs. [6,8]. In this paper, frequencies are rendered dimensionless by scaling with the vertical thermal diffusion time $\tau_v = 51.2$ sec.

The first dynamical state seen in this system as the Rayleigh number is increased above onset, $\epsilon = 0$, consists of pairs of regular, quasilinear wave packets that propagate around the cell in opposite directions [9]. Above $\epsilon \sim 0.002$, a transition to dispersive chaos [4] is seen. This state consists of the erratic appearance of short-lived, spatially localized TW bursts. As ϵ is increased in the dispersive-chaos regime, the bursts persist longer before collapsing, become slightly narrower in space, and exhibit increasing TW amplitudes and decreasing TW phase velocities. Above $\epsilon \sim 0.006$, the spatial locations of successive bursts start to be correlated, probably because of the convective "self-trapping" described recently by Riecke [10].

This evolution towards longer-lived, correlated spatial regions of ever-slower TW's ultimately leads to the persistent region of steady rolls seen in Fig. 1. Remarkably, the rest of the cell is occupied by TW bursts that appear with striking regularity in time. This regularity can be made quantitative by computing temporal spectra from the time series recorded at single spatial points. On top of a broad baseline whose width and center vary with spatial position, these spectra exhibit sharp, regularly spaced lines with spacing denoted ω_{mod}. Here,

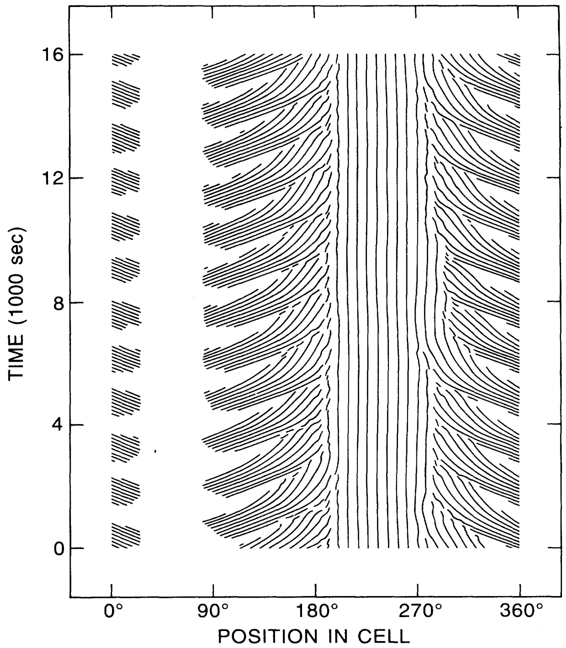

FIG. 1. Coexisting state of TW bursts and steady rolls at $\epsilon=0.012\,12$. In this "phase plot," solid curves show the space-time paths of equal-phase points, which correspond to the boundaries of convective rolls in fully developed convection. In this run, persistent steady rolls (SR's) fill the region between angular locations 190° and 280°. Outside the SR region, TW bursts appear at regular intervals.

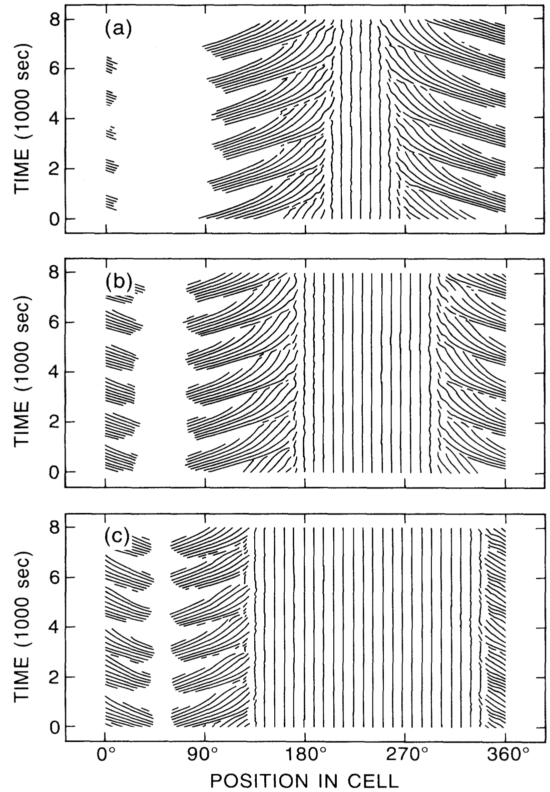

FIG. 2. Evolution of the dynamical state of Fig. 1 with Rayleigh number. (a) $\epsilon=0.011\,31$; (b) $\epsilon=0.012\,93$; (c) $\epsilon=0.015\,35$. With increasing ϵ, the TW region shrinks.

$\omega_{\text{mod}}\sim 0.23$, corresponding to the 1400-sec burst frequency seen in Fig. 1. Importantly, the phase velocity of the TW's in each burst slows considerably as the TW's approach the boundary of the SR region.

Figure 2 shows the evolution of this state with ϵ. The most obvious feature of this dependence is the decrease with ϵ of the length Γ_{TW} of the TW region. As seen in Fig. 3(a), this decrease is approximately linear in ϵ. At sufficiently high Rayleigh number, this evolution fills the cell with spatially uniform, steady rolls.

The regions of steady rolls in the three runs shown in Fig. 2 are centered at the same spatial location. As mentioned above, this is caused by convective "self-trapping": once a SR region is formed, it "digs a hole" in the local ethanol concentration field, which pins it spatially [10]. Subsequent small changes in ϵ, as in the series of experiments in Fig. 2, can change only the size of the region, not its location. However, in experiments in which the pattern was quenched by reducing ϵ far below onset and then remade by increasing ϵ again, the SR region reappeared at apparently random positions. These locations do not seem to be related to fixed inhomogeneities in the convection cell.

The dynamics of the TW bursting exhibits a complex dependence on ϵ and experimental history. As seen in Fig. 3(b), the modulation frequency ω_{mod} decreases as ϵ is increased. More intriguing, in my opinion, is the observation that the left and right TW's can exhibit different bursting frequencies, which I denote $\omega_{L,R}$ [ω_{mod} in Fig. 3(b) is just their average]. In Fig. 1, for example, approximately 12 right-TW bursts and 11 left-TW bursts can be counted. Figure 3(c) shows the difference $|\omega_L-\omega_R|$ between the left- and right-TW burst frequencies, computed from temporal Fourier analysis of the spatially averaged left- and right-TW amplitude profiles. Below $\epsilon\sim 0.015$, these time series exhibit sharp spectral lines at frequencies that differ by fractional amounts ranging from 0.1% to 7%. At $\epsilon=0.015\,35$, the left and right spectral lines are broad and substantially overlap, giving $|\omega_L-\omega_R|=0.001\pm 0.012$. This value is represented by the large error bar without a data point in Fig. 3(c). At $\epsilon=0.016\,50$, the bursts appear so erratically that it is not possible to identify a modulation frequency for either TW component. These data are presumably not reproducible in detail. In particular, $\omega_L-\omega_R$ does not have a consistent sign. This suggests that the left-right modulation-frequency difference is not due to a spatially fixed experimental inhomogeneity.

Figure 4 shows the amplitude profiles of the TW and SR components in the state of Fig. 1 at $\epsilon=0.012\,12$. The SR component was isolated from the raw shadowgraph signal using low-pass temporal filtering. Its amplitude profile was computed at each time step using simple spatial demodulation, and the time average of these profiles is shown as the dotted curve. The temporally oscillating left- and right-TW profiles were computed from the

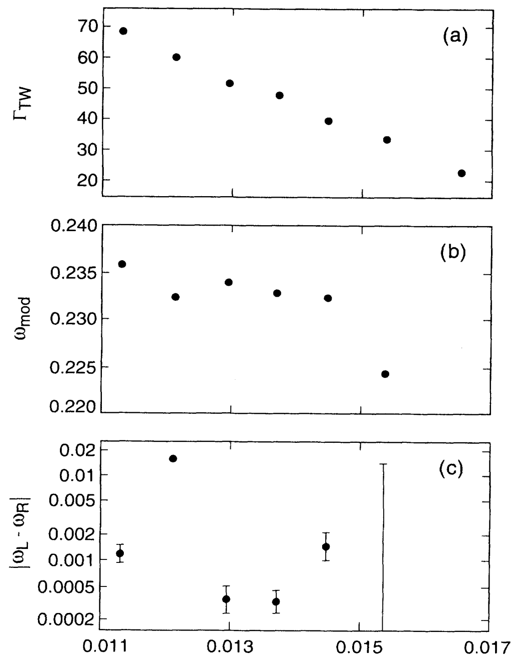

FIG. 3. Quantitative measures of the evolution with increasing Rayleigh number. (a) Length Γ_{TW} of the region in which TW's are seen; (b) average burst frequency $\omega_{mod}=(\omega_L+\omega_R)/2$; (c) difference $|\omega_L-\omega_R|$ between the burst frequencies of the left- and right-TW components. Error bars correspond to the uncertainties in the identification of the centers of spectral lines.

high-pass component of the signal using full complex demodulation [8]. These were then temporally demodulated at ω_{mod} at each spatial point, yielding the time-averaged full and dashed profiles in Fig. 4 (simple time averaging of the TW profiles produced essentially the same curves). The TW profiles seen in this state are reminiscent of the profiles seen in regular blinking states [1],

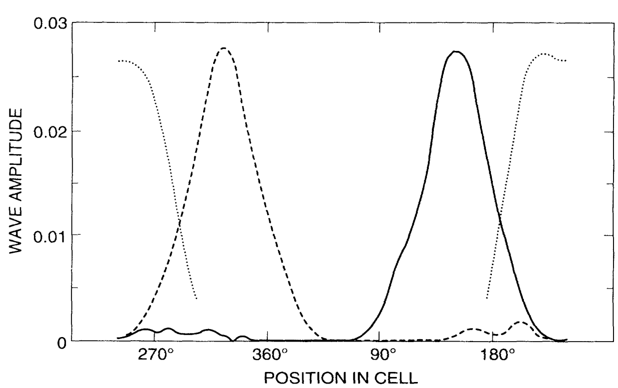

FIG. 4. Time-averaged amplitude profiles for the state of Fig. 1. For clarity, the horizontal axis has been shifted with respect to Fig. 1. Solid curve: right-TW amplitude profile. Dashed curve: left-TW amplitude profile. Dotted curve: SR amplitude profile, reduced in vertical scale by a factor of 5.5 and cut off at low amplitude for clarity. Reflected TW's can be seen at the boundaries of the SR region.

exhibiting the approximately exponential growth in the TW direction that is characteristic of convective instability. The TW amplitudes decay near the edges of the SR region—such "healing regions" are also seen in blinking states [1,2]. In each of the healing regions, the opposite TW component also appears, in a weak, irregularly shaped bump (i.e., the left TW's seen near location 180° and the right TW's seen near location 300°). While it is not directly apparent from the time-averaged representation in Fig. 4, the weak left-TW bump in the right-hand healing region exhibits the same modulation frequency $\omega_R=0.2402$ as the incident right TW. Similarly, both the left TW's incident on the other healing region and the weak right TW's excited there are modulated at $\omega_L=0.2245$. Thus, the weak TW's in the healing regions can be "spectroscopically" identified as *reflections* of the incident TW's from the boundaries of the SR regions. The reflection coefficient is roughly $r\sim 0.1$. The reflected TW's, however, are completely attenuated by the incident TW's.

The observations reported in this paper are unusual in several ways. First, they represent reentrant order beyond a region of chaos. Second, the regularity of the TW bursts is quite striking. Third, the fact that the left- and right-TW bursts appear with different but regular periodicities is also remarkable. Finally, the reflection of TW's from SR's is unprecedented [11]. While the combination of convective instability, nonlinear cross-coupling, and reflecting boundaries constitutes the recipe for regular "blinking" in short rectangular containers [2], the present results are not the same phenomenon. In blinking states seen near onset, the TW amplitudes remain small, as indicated by high TW phase velocities. Because of this, reflected TW's can interact weakly with the incident TW's, tunneling through and ultimately dominating. This leads to the alternating appearance of the opposite TW components, "phase-antilocked" even if irregular. In the present experiments, the severe reduction of phase velocity experienced by the TW's as they approach the SR region is the sign of strong nonlinearity. Because of this, the reflected TW's are totally absorbed and are irrelevant to the process that causes bursting. In this sense, the present experiments have more in common with those of Ref. [5], in which absorbing boundaries were used. In those experiments, convective amplification of TW fluctuations in the center of the cell led to small-amplitude TW's that exhibited irregular blinking. In the present work, because reflected TW's are absorbed, convective amplification of TW fluctuations born in the center of the TW region must also be the source of the dynamics. The chief puzzle presented by these observations is that this process leads to dynamics that are regular, not erratic.

The strong nonlinearity observed in this work would certainly invalidate any attempt at explaining these states in detail using a perturbative, Ginzburg-Landau-equation approach. However, I suggest that the key to the regular appearance of TW bursts lies in the suppression of small-amplitude TW's in the center of the TW region by higher-amplitude, slower TW's encountered downstream. Because of the nonlinear self-interactions, new bursts cannot form coherently in the center of the TW region until higher-amplitude wave packets have propagated sufficiently far away. Thus the growth and propagation of those wave packets set a time scale for bursting. Perhaps a phenomenological model of this process will allow an explanation of the periodic dynamics in the context of a weakly nonlinear theory.

I thank P. C. Hohenberg for a critical reading of this manuscript.

[1] P. Kolodner and C. M. Surko, Phys. Rev. Lett. **61**, 842 (1988); J. Fineberg, E. Moses, and V. Steinberg, *ibid.* **61**, 838 (1988); P. Kolodner, C. M. Surko, and H. Williams, Physica D **37**, 319 (1989); V. Steinberg, J. Fineberg, E. Moses, and I. Rehberg, *ibid.* **37**, 359 (1989).

[2] M. C. Cross, Phys. Rev. A **38**, 3593 (1988); M. C. Cross, Physica D **37**, 315 (1989).

[3] V. Steinberg and E. Kaplan, in *Proceedings of the NATO Advanced Research Workshop on Spontaneous Formation of Space-Time Structures and Criticality,* edited by T. Riste and D. Sherrington (Kluwer, Dordrecht, 1991), p. 207.

[4] P. Kolodner, J. A. Glazier, and H. L. Williams, Phys. Rev. Lett. **65**, 1579 (1990); J. A. Glazier, P. Kolodner, and H. Williams, J. Stat. Phys. **64**, 945 (1991).

[5] W. Schöpf and I. Rehberg, Europhys. Lett. **17**, 321 (1992).

[6] P. Kolodner, Phys. Rev. A **46**, 6431 (1992).

[7] P. Kolodner, H. Williams, and C. Moe, J. Chem. Phys. **88**, 6512 (1988).

[8] P. Kolodner and H. Williams, in *Proceedings of the NATO Advanced Research Workshop on Nonlinear Evolution of Spatio-temporal Structures in Dissipative Continuous Systems,* Vol. 225 of *NATO Advanced Study Institute, Series B2,* edited by F. H. Busse and L. Kramer (Plenum, New York, 1990), p. 73.

[9] P. Kolodner, Phys. Rev. Lett. **69**, 2519 (1992).

[10] H. Riecke, Phys. Rev. Lett. **68**, 301 (1992).

[11] V. Steinberg and E. Kaplan (private communication) have observed reflections of small-amplitude TW's from localized TW structures. Direct observation of end-wall reflections was presented by P. Kolodner, C. M. Surko, A. Passner, and H. L. Williams, Phys. Rev. A **36**, 2499 (1987). The reflection for this process was calculated by M. S. Bourzutschky and M. C. Cross, Phys. Rev. A **45**, 8317 (1992).